Journal of Alloys and Compounds 507 (2010) 456–459

Contents lists available at ScienceDirect

Journal of Alloys and Compounds

journal homepage: www.elsevier.com/locate/jallcom

Synthesis and cathodoluminescence of In_2O_3–SnO_2 nanowires heterostructures

Yinxiao Du*, Pei Ding

Department of Mathematics and Physics, Zhengzhou Institute of Aeronautical Industry Management, DaXue Street, Zhengzhou 450015, China

ARTICLE INFO

Article history:
Received 3 June 2010
Received in revised form 28 July 2010
Accepted 29 July 2010
Available online 4 August 2010

Keywords:
Nanostructured materials
Gas–solid reactions
Optical property

ABSTRACT

Novel In_2O_3–SnO_2 heterostructured nanowires composed of In_2O_3 nanoparticles and SnO_2 nanowires were fabricated via a facile thermal evaporation method. The well crystalline SnO_2 nanowires with average length of 10 μm are first formed, and the In_2O_3 overlayers composed of nanoparticles then are grown on the surface of the SnO_2 nanowires to form the novel In_2O_3–SnO_2 heterostuctures. The In_2O_3 nuclei form in an anisotropic manner during the formation process, which results in the In_2O_3–SnO_2 heterostuctures. All the cathodoluminescence spectra of individual nanowires reveal a strong and broad orange emission band centered at *ca.* 621 nm. It is thought that the integration of the oxygen vacancies of In_2O_3 and SnO_2 is the main reason for the unusual nanowires.

1. Introduction

In the past decades, much effort has been made to study the syntheses and applications of various one-dimensional (1D) nanostructures such as nanotubes and nanowires due to their unique optical, electric and mechanic properties [1–8]. Among various nanowires, 1D heterostructured nanowires have attracted more attentions because the modulated compositions are of multiple functionalities by combining the physical properties of the different materials. Up to now, various synthesis routes including chemical vapor deposition, self-assembly, hydrothermal routes, and template-assisted methods are successfully applied to the synthesis of the heterostructured nanowires which exhibits enhanced properties in nanoelectronics, nanophotonics, sensing and catalysis [9–20]. SnO_2 is one of the most important semiconductors and has been widely used for transparent conductors, gas sensors, solar cells and lithium-ion batteries due to its wide band gap of 3.6 eV at room temperature [21–29]. Intensive researches have focused on the synthesis and application of SnO_2-based heterostructures because SnO_2 can pair with the other materials to form heterojunction that separates the photogenerated electron–hole pair, which results in the enhancement of the performances of the solar cell devices and catalysts [30–33]. Recently, In_2O_3–SnO_2 heterostructured nanowires were found to possess excellent storage capacity and rectifying behaviors compared with the conventional SnO_2 nanowires [34,35]. For example, Kim et al. [35] reported that the electronic conductivity of the individual In_2O_3–SnO_2 heterostructured nanowires was two orders of magnitude better than that of pure SnO_2 nanowires. In this work, we report a facile one-step thermal evaporation method to synthesize novel In_2O_3–SnO_2 heterostructured nanowires. The structure, growth mechanism and cathodoluminescence (CL) properties of the heterostructures are studied in detail.

2. Experimental

The experiments were conducted in a furnace with a quartz tube mounted horizontally inside. High-purity In (99.99%) and SnO (99.99%) with molar ratio of 1:3 were placed in two quartz boats, respectively, and were put into the center of the quartz tube parallel to each other. (1 0 0)Si substrates with 5 nm thick gold coating were placed downstream inside the tube. Prior to heating, the system was evacuated to vacuum (10^{-2} Torr). Then, the tube was heated up to 800 °C and held for 30 min and finally cooled to room temperatures. White products were found to deposit on the Au coated Si substrates. In the whole experiment, a constant flow of O_2 was introduced at a rate of 20 sccm.

The corresponding X-ray diffraction (XRD) pattern was collected from Rigaku X-ray diffractometer (Cu Kα radiation, λ = 1.5418 Å at 40 kV and 160 mA). The morphology of the nanowires was characterized by using field emission scanning electron microscopy equipped with energy-dispersive X-ray spectroscopy (FE-SEM; FEI XL30 S-FEG). The microstructure of the nanowires was further characterized by transmission electron microscope (TEM; Philips CM200). The cathodoluminescence (CL) studies of individual nanowire were performed in the scanning electron microscope equipped with an Oxford Instruments MonoCL2 spectrometer at room temperature.

3. Results and discussion

Fig. 1 shows the XRD patterns of the as-deposited products. The diffraction peaks that are denoted as # and * symbol, respectively, can be indexed as rutile SnO_2 (ICDD-PDF No. 41-1445) and cubic In_2O_3 (ICDD-PDF No. 76-0152). No diffraction peaks from other impurities are detected within the instrumental errors, indicating that the products are only composed of SnO_2 and In_2O_3. The EDS measurement is also used to characterize the composition of

* Corresponding author. Tel.: +86 371 68252171; fax: +86 371 68252171.
E-mail address: dyxiphy@yahoo.cn (Y. Du).

0925-8388/$ – see front matter © 2010 Elsevier B.V. All rights reserved.
doi:10.1016/j.jallcom.2010.07.201

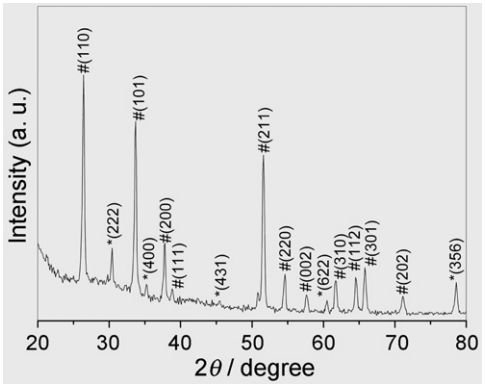

Fig. 1. XRD patterns of the SnO_2–In_2O_3 heterostructured nanowires. # and * denote diffraction peaks of the SnO_2 and In_2O_3, respectively.

the products, as shown in Fig. 2a. Only O, Sn and In elements are detected in the EDS spectrum, which further demonstrates that the products only consist of SnO_2 and In_2O_3. Fig. 2b gives an overview of the product. Large amount of straight nanowires with average length of *ca.* 10 μm are found to deposit on the Si substrates. The enlarged SEM image (Fig. 2c) clearly reveals that irregular overlayer composed of nanoparticles is developed on most of the surface of the nanowires, indicating that the products are maybe of heterostructured nanowires consisted of SnO_2 and In_2O_3.

TEM measurement and EDS spectrum are used to further investigate the microstructures and compositions of the nanowires and overlayers, respectively. As shown in the inset of Fig. 3a, some nanoparticles with regular triangular shapes were grown on the surface of the straight nanowire. Fig. 2b and c was the EDS spectra of a single nanowire and nanoparticle shown in Fig. 2a, respectively. The EDS spectra clearly indicate that Sn and O elements are detected in the nanowire, and In and O elements are found in the nanoparticle. The ratio of O/Sn and O/In are *ca.* 1.931:1 and 1.486:1, respectively, close to the chemical formation of SnO_2 and In_2O_3. The corresponding HRTEM images of the nanowire and nanoparticle (Fig. 3d and e) are indexed to be rutile SnO_2 and cubic In_2O_3, based on the lattice fringes in panels d and e of Fig. 3. These results further demonstrate the heterostructured formation of In_2O_3 nanoparticles-SnO_2 nanowires.

We also investigate the effects of the growth time on the morphology of the heterostructure. Fig. 4a–b shows the TEM images of typical individual nanowires obtained at different grown time with 45 and 60 min, respectively. It is found that an overall In_2O_3 layer with larger thickness was sheathed on the surface of the SnO_2 nanowires at the growth time of 45 min, while the SnO_2 nanowires were completely wrapped with In_2O_3 layer when the growth time is increased to 60 min. It is demonstrated that the In_2O_3 layer will gradually sheath the SnO_2 nanowires with the increase of the growth time, and finally completely wrap the SnO_2 nanowires to form In_2O_3 shell–SnO_2 core formation. The similar In_2O_3–SnO_2 heterostructured nanowires had been reported by Kim et al. [35]. They suggested a detailed mechanism for the adsorption of In_2O_3 on the surface of the SnO_2 nanowires. It is thought that, when the In_2O_3 nuclei reach the thermodynamic size limit, In_2O_3 nuclei will form in anisotropic manner, which is determined by the free energy gain during the growth process. We deduce that the growth mechanism is also applicable to the growth of the heterostructures in this work. In the early growth stage, In_2O_3 nuclei will first and continuously grow in an anisotropic manner, resulting in prism-shaped nuclei on the SnO_2 nanowires. That is the saw-filling growth. If the In_2O_3 nuclei continue to grow in an anisotropic manner, the contiguous nuclei are then transformed into shell satisfying the growth of the In_2O_3 nuclei on the SnO_2 nanowires from the free energy gain viewpoint. So, the complete In_2O_3 shell–SnO_2 core formation will be final formed with increase of the growth time.

Fig. 5a presents the room-temperature CL spectrum of the large area of heterostructures. The spectrum is dominated by a strong and broad orange emission band centered at 621.0 nm. Fig. 5b and c reveals spectra of three individual In_2O_3–SnO_2 heterostructured nanowires, respectively. The spectra have been normalized for comparing the difference in position of emission peaks of these

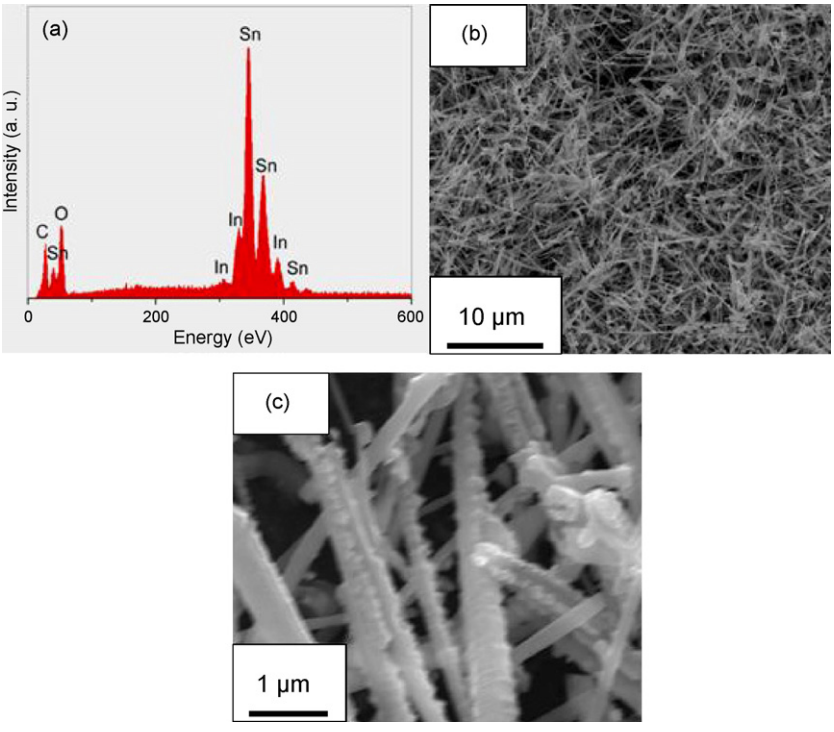

Fig. 2. (a) The EDS spectrum, (b) SEM, and (c) enlarged SEM images of the SnO_2–In_2O_3 heterostructured nanowires.

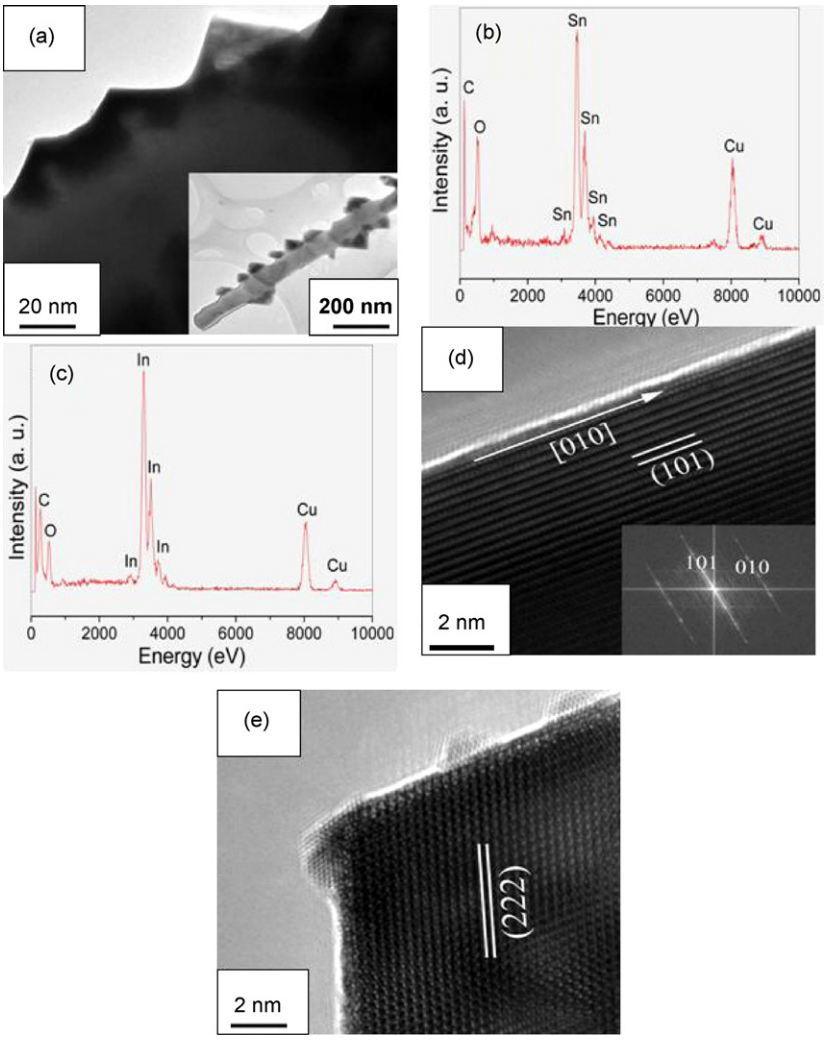

Fig. 3. (a) Enlarged TEM image of an individual SnO_2–In_2O_3 heterostructured nanowires. The inset is TEM image of an individual heterostructure. (b and c) EDS spectra of the regions denoted in (a), respectively. (d) HRTEM image of the nanowire. The inset is FFT pattern of the nanowire. (e) HRTEM image of the nanoparticles.

three spectra. All the spectra indicate similar orange emission properties compared with that of a large area of the heterostructured nanowires. Only the center positions of the emission peaks are slightly different from each other. The minor difference is probably due to the variation of the statistic error induced by the measurement itself. The unusual orange emission band has not been reported in the pure In_2O_3 or SnO_2 semiconductors before. We deduce the unusual orange emission band is the integration of the defect-related emission of In_2O_3 and SnO_2, and oxygen vacancies may be main reason for the unusual emission. The synthesis of the heterostructures is under the oxygen-deficient experiment condition, thus the oxygen vacancies are common in the heterostructures. So, the unusual orange emission band may be originated from the oxygen vacancies existing in the In_2O_3 and SnO_2. However, the exact mechanism for the unusual emission is unknown and needs to be further investigated.

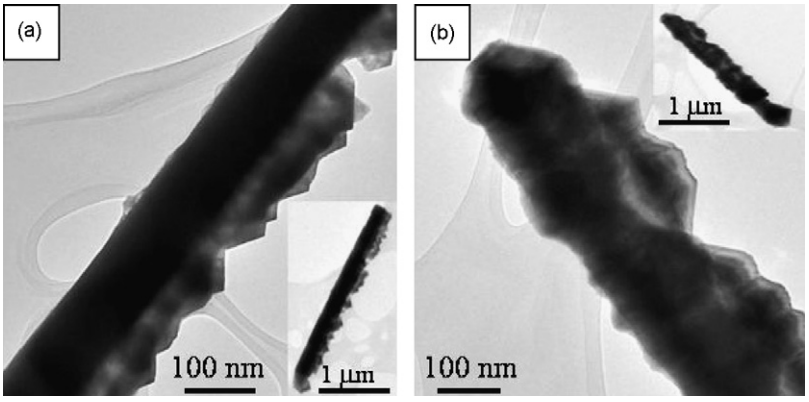

Fig. 4. TEM images of typical individual nanowires obtained at different grown time: (a) 45 min and (b) 60 min.

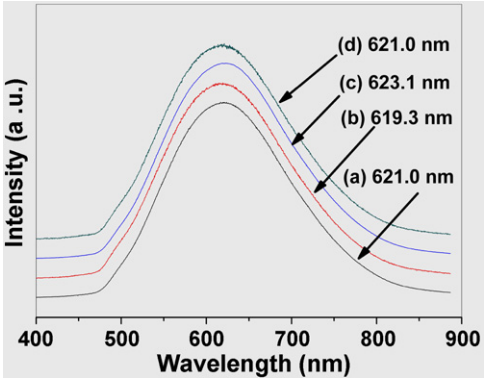

Fig. 5. Room-temperature CL spectra of (a) the large area of heterostructures and (b–d) three different individual heterostructures.

4. Conclusions

We develop a facile thermal evaporation method to fabricate novel In_2O_3–SnO_2 heterostructured nanowires. The heterostructures are composed of In_2O_3 nanoparticles and SnO_2 nanowires. The well crystalline SnO_2 nanowires with average length of 10 μm were first formed, and then the In_2O_3 nanoparticles with average size of 30 nm are grown on the surface of the SnO_2 nanowires to form the novel In_2O_3–SnO_2 heterostuctures. The thickness of the In_2O_3 layer sheathed on the surface of the SnO_2 nanowires is gradually increased with the increase of growth time, and finally the SnO_2 nanowires are completely wrapped in In_2O_3 layer to form In_2O_3 shell–SnO_2 core formation. It is found that the anisotropic manner of In_2O_3 nuclei results in unusual In_2O_3–SnO_2 heterostructures. All the CL spectra of individual nanowires reveal a strong and broad orange emission band. It is deduced that the integration of the oxygen vacancies of In_2O_3 and SnO_2 should be responsible for the unusual orange emission of the heterostructures.

Acknowledgements

This work was financially supported by the Natural Science Foundation of Henan Provincial Educational Department (No. 2010B140015), and the Aeronautical Science Foundation of China (No. 2008ZF55006).

References

[1] C. Kocabas, S. Dunham, Q. Cao, K. Cimino, X.N. Ho, H.S. Kim, D. Dawson, J. Payne, M. Stuenkel, H. Zhang, T. Banks, M. Feng, S.V. Rotkin, J.A. Rogers, Nano Lett. 9 (2009) 1937–1943.
[2] M. Lei, H. Yang, P.G. Li, W.H. Tang, Appl. Surf. Sci. 254 (2008) 1947–1952.
[3] Y.B. Tang, Z.H. Chen, H.S. Song, C.S. Lee, H.T. Cong, H.M. Cheng, W.J. Zhang, I. Bello, S.T. Lee, Nano Lett. 8 (2008) 4191–4195.
[4] H. Liu, D. Wexler, G.X. Wang, J. Alloys Compd. 487 (2009) L24–L27.
[5] X.D. Wang, J.H. Song, J. Liu, Z.L. Wang, Science 316 (2007) 102–105.
[6] M. Lei, H. Yang, Y.F. Guo, B. Song, P.G. Li, W.H. Tang, Mater. Sci. Eng. B 143 (2007) 85–89.
[7] P.X. Cao, Y. Ding, Z.L. Wang, Nano Lett. 9 (2009) 137–143.
[8] M. Lei, H. Yang, P.G. Li, W.H. Tang, J. Alloys Compd. 459 (2009) 338–342.
[9] J. Cao, J.Z. Sun, H.Y. Li, J. Hong, M. Wang, J. Mater. Chem. 14 (2004) 1203–1206.
[10] T. Tan, Y. Li, Y. Liu, B. Wang, X.M. Song, E. Li, H. Wang, H. Yan, Mater. Chem. Phys. 111 (2008) 305–308.
[11] M. Lei, L.Q. Qian, Q.R. Hu, S.L. Wang, W.H. Tang, J. Alloys Compd. 487 (2009) 568–571.
[12] Y.J. Hsu, S.Y. Lu, Chem. Commun. 18 (2004) 2102–2103.
[13] Y. Tak, H. Kim, D. Lee, K. Yong, Chem. Commun. 38 (2008) 4585–4587.
[14] N.W. Wang, Y.H. Yang, G.W. Yang, J. Phys. Chem. C 113 (2009) 15480–15483.
[15] L. Ouyang, K.N. Maher, C.L. Yu, J. McCarty, H. Park, J. Am. Chem. Soc. 129 (2007) 133.
[16] C.H. Lee, J. Yoo, Y.J. Doh, G.C. Yi, Appl. Phys. Lett. 94 (2009) 043504.
[17] A.J. Mieszawska, R. Jalilian, G.U. Sumanasekera, F.P. Zamborini, Small 3 (2007) 722–756.
[18] H.W. Kim, H.S. Kim, H.G. Na, J.C. Yang, C. Lee, J. Alloys Compd. 500 (2010) 175–180.
[19] L.Q. Qian, S.J. Wang, X. Jia, Y.Y. Liu, W.H. Tang, J. Alloys Compd. 477 (2010) 888–891.
[20] X.H. Huang, Y.W. Yang, X.C. Dou, Y.G. Zhu, G.H. Li, J. Alloys Compd. 461 (2008) 427–431.
[21] A. Umar, J. Alloys Compd. 485 (2009) 759–763.
[22] P.H. Wei, G.B. Li, S.Y. Zhao, L.R. Chen, J. Electrochem. Soc. 146 (1999) 3536–3537.
[23] P.G. Li, M. Lei, W.H. Tang, X. Guo, X. Wang, J. Alloys Compd. 477 (2009) 515–518.
[24] G. Faglia, C. Baratto, G. Sberveglien, M. Zha, A. Zappettini, Appl. Phys. Lett. 86 (2005) 011923.
[25] J.H. Ahn, Y.J. Kim, G.X. Wang, J. Alloys Compd. 483 (2009) 422–424.
[26] M. Lei, Q.R. Hu, S.L. Wang, W.H. Tang, Mater. Lett. 64 (2010) 19–21.
[27] Q. Kuang, C.L. Lao, Z.L. Wang, X. Xie, L.S. Zheng, J. Am. Chem. Soc. 129 (2007) 6070–6071.
[28] P.G. Li, X. Guo, X.F. Wang, W.H. Tang, J. Alloys Compd. 479 (2009) 74–77.
[29] V.V. Sysoev, J. Goschnick, T. Schneider, E. Strelcov, A. Kolmakov, Nano Lett. 7 (2007) 3182–3188.
[30] Q. Kuang, Z.Y. Jiang, Z.X. Xie, S.C. Lin, Z.W. Lin, S.Y. Xie, R.B. Huang, L.S. Zheng, J. Am. Chem. Soc. 127 (2005) 11777–11784.
[31] I.E. Titkov, I.P. Pronin, E.Y. Kaptelov, L.A. Delimova, I.A. Liniichuk, I.V. Grekhov, Phys. Solid State 51 (2009) 1538–1540.
[32] L.J. Lauhon, M.S. Gudiksen, C.M. Lieber, Philos. Trans. R. Soc. London, Ser. A 362 (2004) 1247–1260.
[33] J.X. Wang, H.Y. Chen, Y. Gao, D.F. Liu, L. Song, Z.X. Zhang, X.W. Zhao, X.Y. Dou, S.D. Luo, W.Y. Zhou, G. Wang, S.S. Xie, J. Cryst. Growth 284 (2005) 73–79.
[34] A. Vomiero, M. Ferroni, E. Comini, G. Faglia, G. Sberveglieri, Nano Lett. 7 (2007) 3553–3558.
[35] D.W. Kim, I.S. Hwang, S.J. Kwon, H.Y. Kang, K.S. Park, Y.J. Choi, K.J. Choi, J.G. Park, Nano Lett. 7 (2007) 3041–3045.